Rheological Characterization and Morphology of Nylon 1212/Functional Elastomer Blends

Wanjie Wang,[1] Yanxia Cao,[1] Jingwu Wang,[1] Qiang Zheng[2]

[1]*College of Materials Science and Engineering, Zhengzhou University, Zhengzhou 450001, China*
[2]*Department of Polymer Science and Engineering, Zhejiang University, Hangzhou 310027, China*

Received 19 May 2008; accepted 8 October 2008
DOI 10.1002/app.29459
Published online 23 January 2009 in Wiley InterScience (www.interscience.wiley.com).

ABSTRACT: The rheological characterization and morphological analysis of nylon 1212 toughened with a maleated triblock copolymer styrene-*b*-(ethylene-*co*-butylene)-*b*-styrene (SEBS-*g*-MA) elastomer were carried out. We found that the critical shear strain of nylon 1212 was higher than that of virgin SEBS-*g*-MA and the plateau modulus of the blends in the curves of a dynamic strain sweep test was larger than those of the virgin components. All of the curves of a dynamic frequency sweep test showed a second plateau in the low-frequency region, except those of nylon 1212 and the blend containing 10 wt % SEBS-*g*-MA. Furthermore, the positive deviation in the plots of G' versus blend composition demonstrated that the blends were still immiscible, although the graft reaction improved the compatibility of the blends. According to the theory of phase transition, the phase-inversion point was predicted to be about 50 wt % SEBS-*g*-MA, which corresponded to the morphology analysis. Additionally, the yield stress behaviors and long-time relaxation behaviors of the blends were investigated. © 2009 Wiley Periodicals, Inc. J Appl Polym Sci 112: 953–962, 2009

Key words: blends; elastomers; nylon; rheology

INTRODUCTION

Blending is one of the most available and effective ways to modify the properties of polymers; it can improve the workability of a given material with new and modified properties. As a result, a lot of complex polymeric materials have been developed for different requirements.[1–3] It is well known that only a few polymers are miscible on a molecular level, and most polymers are immiscible and incompatible. The compatibility between immiscible polymers can be enhanced through the addition of a third component (a so-called compatibilizer) or *in situ* chemical reactions between blend components (reactive blending). The latter is a comparatively new method, which relies on the *in situ* formation of copolymers or the interaction of polymers in the melt blends without the addition of a separate compatibilizer. This route has been used to produce blends of polycarbonate and polyesters, toughened polymers with reactive end groups, and so on.[4–10] In general, polymeric materials of high toughness are usually acquired through the blending of engineering plastics with suitable functional elastomeric materials, which has become one of the most popular methods for improving the toughness of a brittle polymer. The degree of toughness is determined by the blending ratio, the size of phase domain, the interaction between the matrix and elastomer, the blending approaches, processing parameters, and so on.[11–15]

Long-chain nylons, such as nylon 11, nylon 12, and nylon 1212, have been widely used in machinery, electronic equipment, automobiles, and the information and aviation industries. It is well accepted that these polymers give superior properties because they provide a combination of high strength and toughness, abrasion resistance, and dimensional stability. Compared to nylon 11 and nylon 12, the mechanical properties of nylon 1212 have been improved with its other properties kept almost unchanged.[16] Moreover, abundant and cheap raw materials and low production costs make nylon 1212 competitive. It seems that nylon 1212 could replace nylon 11 and nylon 12 in many application fields. However, in some special cases, the toughness of nylon 1212 could hardly satisfy the requirements. Hence, it is necessary to toughen nylon 1212. It is well known that one of the end groups of nylon 1212 is amine, which is capable of reacting with other groups; therefore, in this study, a functional elastomer was used as a kind of toughener to blend with nylon 1212 to acquire a high-toughness nylon material.

In the past 2 decades, a lot of studies of nylon/functional elastomer blends have been mostly

Correspondence to: W. Wang (wwj@zzu.edu.cn).
Contract grant sponsor: Henan Province Fundamental and Advanced Technology Research Projects; contract grant number: 072300440030.

concerned with the aspects of mechanical and thermal properties.[17–23] To our knowledge, few reports have dealt with the rheological behaviors of their melts.[24–26] The rheological measurements not only give much useful information on material molding and processing but also provide an effective approach to characterize the structure and properties of polymer materials.[27,28] The processability of polymers is directly related to the rheological behaviors, and for homopolymers, the rheological behaviors depend mainly on chain and agglomeration structure. In the case of polymer blends, the rheological behaviors are involved in not only the original properties but also phase morphology, interaction in the interface, and so on. Obviously, it is considerably complex to probe the essence of the rheological behaviors of polymeric blends. The linear viscoelastic behaviors of polymers and their blends have attracted the ever-increasing interest of researches, and the correlations of their microstructure and linear viscoelastic behavior have been reported.[29–33] The aim of this study was to investigate the rheological characterization of nylon 1212/functional elastomer blends and probe the mechanism of long-time relaxation and the relationship between the rheological behaviors of the blends and their morphologies.

EXPERIMENTAL

Materials

The nylon 1212 (melt flow index = 22.43 g/min under 5.0 kg of pressure at 230°C, melting point = 184°C, glass-transition temperature = 46°C, relative density = 1.01) used in this study was a product of Shandong Dongchen Engineering Plastic Co., Ltd. (Houston, USA) (Qingdao, China). The maleated triblock copolymer styrene-*b*-(ethylene-*co*-butylene)-*b*-styrene (SEBS-*g*-MA; Kraton FG 1901) was a product of Shell Chemical Co., contained 29 wt % styrene, and had number-average molecular weights of 7500 in the polystyrene blocks and 37,500 in the polyolefin blocks. The weight percentage of MA grafted onto this elastomer was 1.7–2.0 wt %. The antioxidant (B215, relative molecular weight = 647, melting temperature = 453–458 K) was a product of Ciba–Geigy Co. (Basel, Switzerland).

Preparation of the samples

Nylon 1212, SEBS-*g*-MA, and 1 wt % antioxidant were blended in a Haake torque rheometer (Rheoflixer Polylab) [Schwerte, Germany] at 190°C for 10 min. The samples were compression-molded at 190°C into disks 25 mm in diameter and 1.2 mm in thickness.

Measurements

Melt rheological tests were conducted on an Ares Rheometer (Rheometrics, Inc., Piscataway, USA) in parallel-plate oscillatory mode. The dynamic frequency (ω) sweep test was performed from 0.01585 to 100 rad/s, and the strain amplitude was maintained at 1% to ensure that the rheological behavior was located in the linear viscoelastic region. The dynamic strain sweep test was performed from 0.01 to 100%, and the frequency amplitude was maintained at 1 rad/s. Long-stress relaxation tests were performed to record the relaxation modulus with time; the amplitude was 1%, and the test time was 10,000 s. All the tests were performed at 190°C.

The morphologies of the blends were observed with a JSM-5510LV scanning electron microscope (Tokyo, Japan). All samples were fractured in liquid N_2 and etched in boiling xylene for 12 h to remove the nonreactive elastomer of the blends. The etched surface was coated with a conductive gold layer before scanning electron microscopy (SEM) analysis.

RESULTS AND DISCUSSION

Dependence of the viscoelastic behavior on the shear strain (γ)

Figure 1 presents the effects of γ on the dynamic storage modulus (G') and loss modulus (G'') for nylon 1212 and the elastomer. For nylon 1212, it was clear that, in the case of $\gamma \leq 25\%$, G' was independent of γ; this was defined as the linear viscoelastic region. Although $\gamma \geq 25\%$, G' decreased with increasing γ and gave rise to nonlinear viscoelastic behavior.[34] When γ was higher than the critical shear strain of nylon 1212(γ_C), G' no longer exhibited the plateau but fell quickly. The reason for this

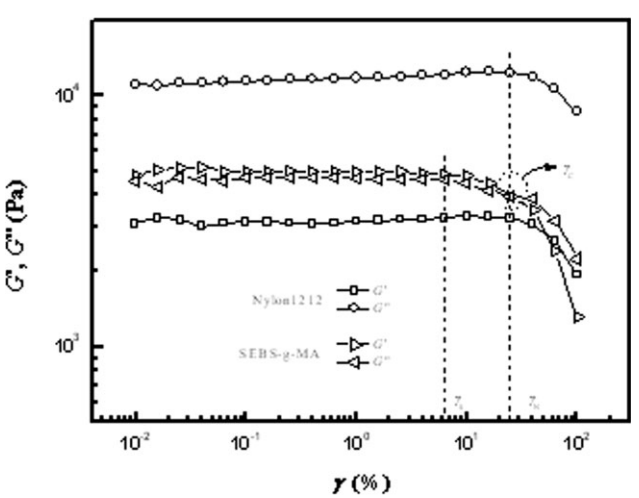

Figure 1 Effect of γ on G' and G'' of nylon 1212 and SEBS-*g*-MA.

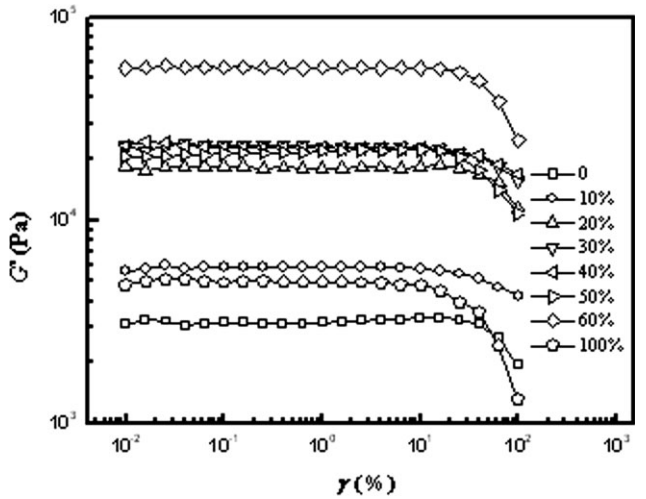

Figure 2 Effect of γ on G' of nylon 1212 and SEBS-*g*-MA blends.

phenomenon was that the velocity of macromolecular disentanglement increased with increasing γ. In other words, when the disentanglement and entanglement were in dynamic equilibrium, G' exhibited a plateau, whereas when the disentanglement dominated over the entanglement, the temporary crosslink points were destroyed, which resulted in a quick decrease in G' because of macromolecular chain slippage and modification of the microstructure along the direction of applied strain.

On the other hand, a much greater reduction in the amplitude of G' was found compared to that of G'', which indicated that G' was more sensitive to γ than G'', which demonstrated that the analysis of the dynamic strain sweep process was relatively reasonable because G' was responsible for elasticity and G'' corresponded to the viscosity. Furthermore, the curve of G'' was located over that of G', which implied that the viscoelastic behavior of nylon 1212 was dominated by the viscosity. As for SEBS-*g*-MA, it was obvious that the curves of G' and G'' showed similar changes, but the critical shear strain of SEBS-*g*-MA (γ_S) was about 6%, which was lower than that of nylon 1212. These results demonstrate that the viscoelastic parameters of the functional elastomer were more sensitive to γ than those of nylon 1212. It is well known that the structure of the styrene block copolymer is a microphase separation structure and belongs to a heterogeneous structure, which is more easily destroyed by an accumulative strain history. Furthermore, the plateau modulus of G' was slightly larger than that of G'', which indicated high elasticity and thermoplasticity of the elastomer. In addition, the curves of G' and G'' intersected at $\gamma_C = 24\%$, which implied that the nonlinear viscoelastic behavior had a transition from elasticity to viscosity with increasing γ the shear strain.

Figure 2 shows the effects of γ on G' of the nylon 1212 and SEBS-*g*-MA blends. G' of the blends showed a modulus plateau in the low-γ range and decreased with increasing γ in the high-γ ranges; this was similar to the G'–γ (%) variations of nylon 1212 and SEBS-*g*-MA. Second, it was clear that the plateau moduli of the blends were higher than those of the virgin components, which did not corresponded to the rules of immiscible blends because the plateau modulus is related to the entanglement molecular weight and phase structure. It is well known that one of the end groups of nylon 1212 is amine, which is capable of reacting with the maleic anhydride groups in the SEBS-*g*-MA and can form copolymers at the interface of the blends (Scheme 1).[35,36] Because of the grafting reaction, the interfacial tension between the blend components decreased, which, in turn, decreased the coalescence and enhanced the phase compatibility. The graft reaction enlarged the length of macromolecular chains, and this effects could not only be seen from the data of the plateau modulus but also from the critical shear strain values of blends, which increased to some degree compared with those of the virgin SEBS-*g*-MA. At a fixed strain, say at 10% strain, the plateau modulus versus blend composition could be plotted; this showed a sigmoid shape of the increase of modulus with composition. The randomness of the grafting reaction in the melt state could have been the reason.

Dependence of the viscoelastic behavior on the frequency

Figure 3 shows the G' and G'' variation with ω for nylon 1212/SEBS-*g*-MA blends containing different amounts of functional elastomer. The viscoelastic behaviors of virgin nylon 1212 and SEBS-*g*-MA were obviously different, but the viscoelastic behaviors of the blends were related to the components of the blends. The virgin nylon 1212 seemed to obey the linear viscoelasticity models, that is, $G' \propto \omega^2$, $G'' \propto \omega$ at low ω, to log $G' \propto 2$ Log ω and log $G'' \propto$ log ω;

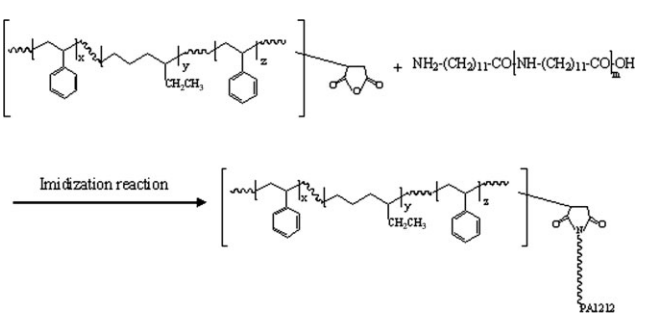

Scheme 1 Graft reaction between nylon 1212 and SEBS-*g*-MA.

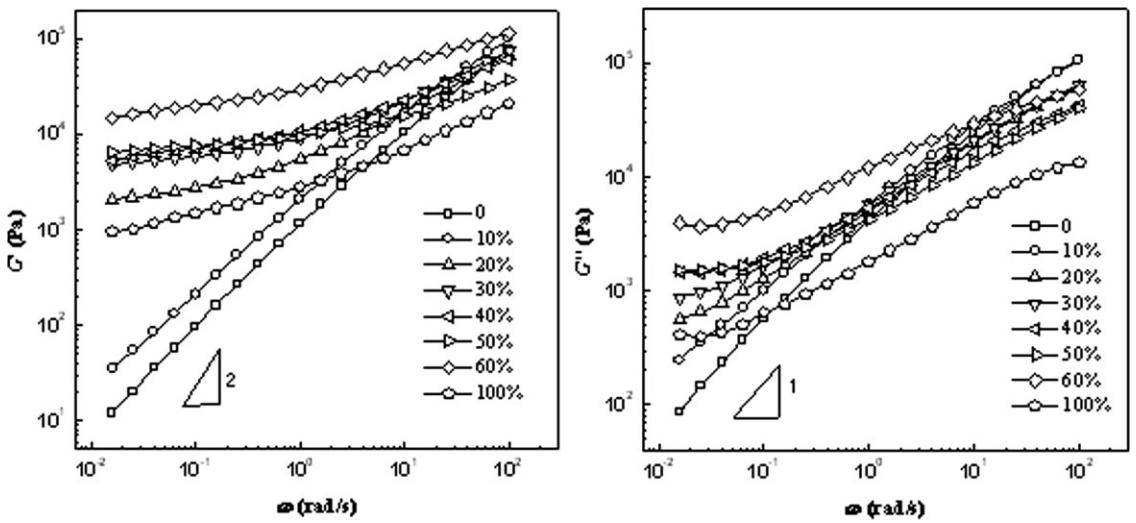

Figure 3 Relationship between G' and G'' with ω for nylon 1212/SEBS-*g*-MA blends.

whereas the blends did not.[37] These were in agreement with the results for other blends systems.[38] Whether the slope of the plot of log $G' \propto$ log ω at low ω was close to 2 or not is in general used as a criterion for examining whether a heterogeneous (or homogeneous) structure in a multicomponent polymer system exists or not. On the other hand, for SEBS-*g*-MA, the curve of $G' \sim \omega$ appeared as an obvious second plateau in the terminal region. In rheology, this phenomenon is thought to be responsible for the emergence of phase separation and the existence of ordered structures, such as agglomerations, skeletons, and networks, to some extent. Additionally, the molecular weight distribution is an important factor that affects the dynamic rheological behavior in the terminal region. In the case of SEBS-*g*-MA, its structure was similar to the structure of SEBS except for the soft block. From macromolecular chain entanglement theory, the hard blocks (polystyrene) act as entanglement points and form a network structure, which results in the topology restraint of the movement of macromolecular chains. It is believed that the microphase separation structures formed from the dynamic process discussed previously induced the emergence of a second plateau in the G'–ω curve.

In the absence of strong interaction between the components, the dynamic rheological behavior of blends is mainly dependent on the matrix and the viscoelastic behavior; that is, the shapes of the curves of the blends should be similar to that of the matrix. In the case of the nylon 1212/SEBS-*g*-MA blends, the blend with 10 wt % SEBS-*g*-MA had similar viscoelastic behavior to that of nylon 1212, whereas the other blends showed mainly the rheological behavior of SEBS-*g*-MA and possessed the second-plateau phenomenon in the bottom of the G'–ω curves, which was attributed to the entanglement of longer macromolecular chains formed through the graft reaction. However, when the content of SEBS-*g*-MA was higher than 10 wt %, all of the G'–ω curves of the blends were almost parallel in the low-frequency range, and G' increased with the content of SEBS-*g*-MA. The G'–ω curves of the blends with 30, 40, and 50 wt % SEBS-*g*-MA were close to each other, which perhaps implies that there were some transition in the phase morphology.

As shown in Figure 3, G'' of the blends displayed a more complex behavior. At low ω, G'' of the blends increased monotonically with SEBS-*g*-MA concentration, and all of the curves of the blends were located over those of pure nylon 1212. Furthermore, the shapes of the log G'' versus log ω curves of the blends were concave, which indicated that a minimum of dissipated energy existed at very low ω. This tendency to form a minimum in the G''–ω curve was greatly pronounced for the blends with high contents of SEBS-*g*-MA. At high frequencies, although the G'' values of all of the blends and pure nylon 1212 were higher than that of SEBS-*g*-MA, it did not exhibit monotonical change with blend composition. It is well known that G' is related to the elastic behavior of the material and is considered the amount of stored energy, whereas G'' represents the amount of dissipated energy. The dependence of G' and G'' on ω reflects the relative motion of all macromolecules in the bulk and can give important information on the rheological behavior of melts. Therefore, we concluded that SEBS-*g*-MA was much more elastic than nylon 1212, and the difference between them increased with decreasing ω. Also, the increase in G' demonstrated that the blends were more elastic than virgin nylon 1212 and SEBS-*g*-MA, which implied the SEBS-*g*-MA elastomer could toughen the nylon 1212 effectively.

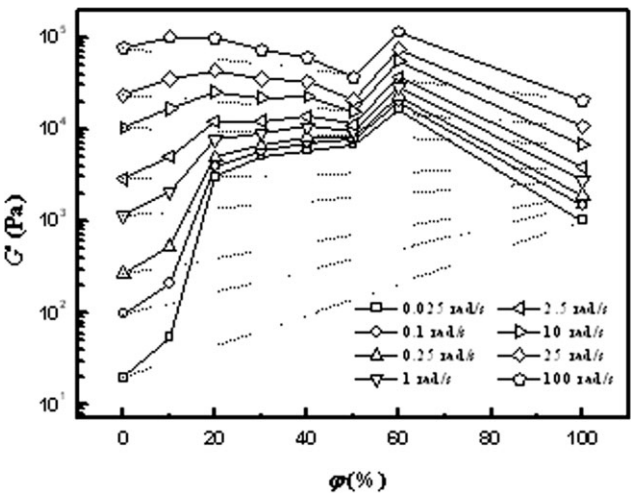

Figure 4 Dependence of G' on the concentration for SEBS-*g*-MA for nylon 1212/SEBS-*g*-MA blends at different frequencies.

Determination of the phase transition

For two-phase blends, the composition dependence of viscoelastic functions gives much information on the level of miscibility of the blended material. It is believed that the shape of the plots of the rheological functions versus composition and their maxima/minima are related to the morphologies of the materials at composition ratios, phase interactions, interfacial tension, and hydrodynamic effects. The method of blend preparation and the type of forming operation are among other parameters controlling the observed interactions between melt-state or solid-state morphology and rheology. Phase inversion, droplet size and shape, cocontinuity, and conversion of droplets into fibrils with different degrees of alignment depending on stress level are all parameters that have been suggested to be responsible for the shape of rheological curves.[39]

The viscoelastic functions of the miscible blends usually follow the log-additivity rule[40,41]:

$$\log F_b = w_m \log F_m + w_d \log F_d \quad (1)$$

where F is a viscoelastic function, w is the weight fraction, and the subscripts b, m, and d indicate the values for the blend, the matrix, and the dispersed phase, respectively. However, there exists some deviations from the log-additivity rule for immiscible blends, in which immiscible polymer blends can be divided into three categories, that is, positive deviation, negative deviation, and positive–negative deviation, on basis of the blend-composition dependence of the viscoelastic function.

Figure 4 presents the dependence of G' on the concentration of SEBS-*g*-MA for the nylon 1212/SEBS-*g*-MA blends at different ω's. G' of the blends showed positive deviations, and the deviations increased with decreasing ω. The reasons for these are that nylon 1212 had a relatively short characteristic relaxation time; consequently, it contributed to the viscoelastic behaviors mainly in the high-ω region. In contrast, the SEBS-*g*-MA, with a microphase separation structure, showed a long characteristic relaxation time, which dominated the viscoelastic behaviors in the low-ω region. Both components in the blends could hardly keep the same response to the external stimulation. At high ω (>10 rad/s), with increasing concentration of SEBS-*g*-MA, the curves of the G' versus composition of the blends showed a peak, which demonstrated that there were some changes in the interaction of the macromolecular chains. The concentration of SEBS-*g*-MA corresponding to the peak was about 20 wt %. Therefore, we inferred that the graft copolymer not only improved the compatibility of the blends but also made the system exhibit a strong response to external stimulation. When the concentration of SEBS-*g*-MA was about 20 wt %, nylon 1212 was the matrix, and the cooperating interaction between nylon 1212 and the graft copolymer was stronger than that of the other blends, which led to a peak at the high-ω curves. In the low-ω region, no peak in the curves emerged, but there was a transition point when the concentration of SEBS-*g*-MA was 20 wt %. G' increased greatly with increasing the concentration for SEBS-*g*-MA (φ) before the transition point, which implied that the degree of graft reaction became large with φ and the concentrations of the graft copolymer improved gradually because the graft copolymer could improve the compatibility of the blends and enhance the degree of entanglement. Although φ was higher than 20 wt %, the increasing amplitude of G' became small, which showed that the degree of graft reaction changed a little with increasing φ. On the other hand, as also shown in Figure 4, the curves of G'–φ at high ω showed a valley, and other curves at low ω exhibited another transition point when φ was about 50%. This valley or transition point should have corresponded to the phase-transition point, which was corroborated in the SEM micrographs.

Figure 5 shows the relationship between the complex viscosity [η*(ω)] and complex modulus [G^*(ω)] for the nylon 1212/SEBS-*g*-MA blends. Such curves are important for examining yield stress behavior,[42] even though they can hardly be observed in some miscible blends. A sharp upturn in η*(ω) at low G^*(ω) indicated the existence of yield stress, which generally exists in immiscible and filled polymer systems. A sharp increase in η*(ω) as G^*(ω) decreased seemed to be indicative of the existence of yield stress in SEBS-*g*-MA, which resulted from the microphase separation structure. As for the virgin nylon 1212, η*(ω) approached a constant value with increasing G^*(ω) and exhibited Newtonian behavior

at low ω. Compared to nylon 1212 and SEBS-*g*-MA, the blends with 10 wt % SEBS-*g*-MA showed similar behavior to nylon 1212, but other blends showed yield stress behavior, although the graft reaction between bottom groups could stabilize the interface by reducing the coalescence and interfacial tension and improving the compatibility of the blend components.

Figure 6 presents a comparison of the curves of G' versus G'' for different compositions of the nylon 1212/SEBS-*g*-MA blends. Plots of G' versus G'', that is, so-called Cole–Cole plots of modulus, were used by Han and coworkers[43,44] to investigate the miscibility of polymer blends; they suggested that plotting G' against G'' gives rise to correlations that may become independent of blend composition for compatible blend systems but dependent on blend composition for incompatible blend systems. Furthermore, the increase in G' could be attributed to the entanglement in the compatibilized blend, and certain rheological parameters, such as G', G'', and η*, could be used to determine compatibility. The change in the microstructure of the blends and the compatibility of the polymers could also be predicted from the curves of $G' \sim G''$.[43,44]

It is well known that there exists chemical interaction between nylon 1212 and SEBS-*g*-MA. The graft copolymer formed by chemical interaction always has been dispersed in the interface between two phases, which reduces the interfacial tension and improves the compatibility. However, curves of each blend with a different blend ratio exhibited a strong dependence on blend composition, which demonstrated that these blends were incompatible (Fig. 6). Obviously, the reason for this can be attributed to morphological changes accompanying the change in composition. Therefore, we concluded that the graft ratio was relatively low, which led to inferior compatibility of the blend components. Furthermore, as also shown in Figure 6, the curve of virgin nylon 1212 seemed to be a straight line, and the curve of the blend with 10 wt % SEBS-*g*-MA had a similar shape. However, the shapes of the curves with 20–30 wt % SEBS-*g*-MA were not similar to that of the virgin nylon 1212 and had an upturn in the low-ω region, and other curves showed transition points. The differences in the shapes of the curves meant that the addition of SEBS-*g*-MA changed the melt flow behavior of nylon 1212. Additionally, the curves of the blends were located to the left side of that of nylon 1212, which indicated that the addition of functional elastomer enhanced the elasticity of the blends and changed the processing properties.

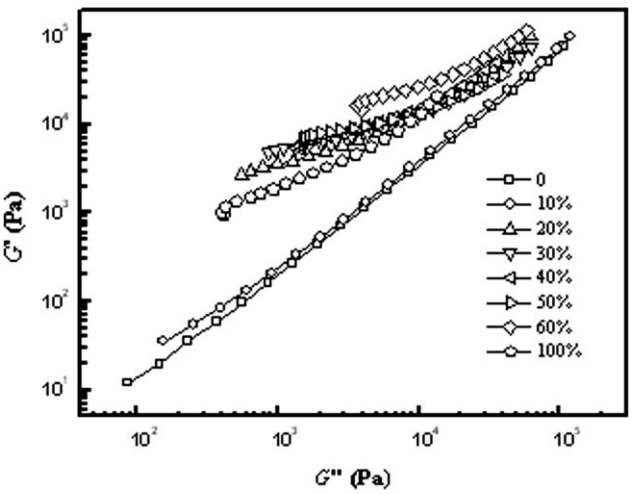

Figure 6 Relationship between G' and G'' for nylon 1212/SEBS-*g*-MA blends.

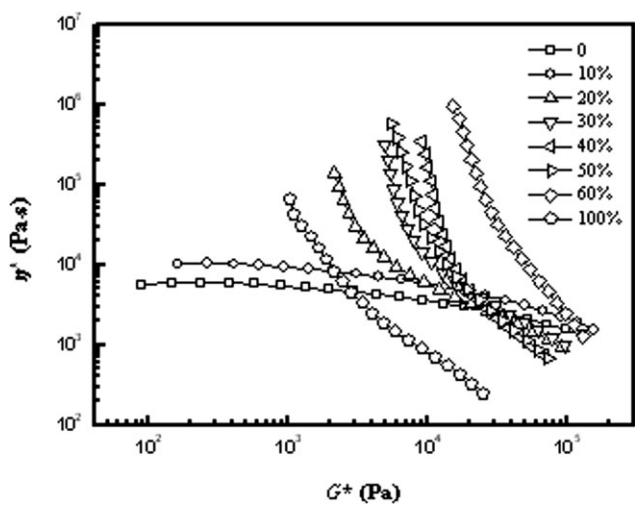

Figure 5 Relationship between η* and G^* for nylon 1212/SEBS-*g*-MA blends.

Long-time relaxation behaviors of blends

Figure 7 presents the long-time relaxation curves of the nylon 1212/SESB-*g*-MA blends and their fits by the Ninomiya equation and Maxwell model. The two pure components exhibited completely different relaxation behaviors. The virgin nylon 1212 demonstrated a fast relaxation process, whereas the virgin SEBS-*g*-MA first exhibited fast and then slow relaxation processes. The fast relaxation of SEBS-*g*-MA corresponded to the relaxation behavior of a hard block (polystyrene), whereas the slow one was endowed with the block random copolymer. However, the trail of the relaxation modulus [$G(t)$] for nylon 1212 became too small and led to slight scattering on the results. This was because the measured torque was below the lower limitation of the transducer. On the other hand, the curve of the pure functional elastomer showed a relaxation plateau in the long-time region, which perhaps corresponded to the second plateau emerging in the curve of the ω sweep at low

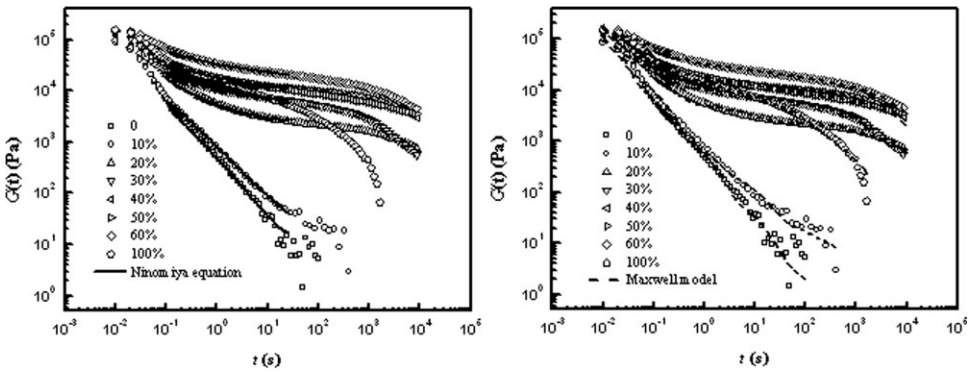

Figure 7 Long-time relaxation curves of nylon 1212/SEBS-*g*-MA blends and their fits with the Ninomiya equation and Maxwell model.

ω values (Fig. 3). As for the blends, the relaxation behaviors of the blends with high contents of elastomer were that of pure functional elastomer, whereas for the blend with 10 wt % elastomer, the relaxation behaviors were qualitatively similar to that of the virgin nylon 1212. In the long-time region, all of the curves of the blends, except the blend with 10 wt % elastomer, were located over those of the pure components, which were completely different than those of immiscible polymer blends. Furthermore, there were more obvious relaxation plateau for the blends with high contents of elastomer than for the pure functional elastomer, and the values of the relaxation plateau for some blends were higher than that of the pure functional elastomer. The reasons for these were that the graft reaction between the pure components enlarged the length and changed the entanglement density of the macromolecular chain. The different molecular structure and phase morphologies led to special relaxation modes and relaxation strength.

For further evaluation of the linear viscoelastic behavior of the blends at small γ, the Ninomiya and Ferry equation was used to calculate $G(t)$ from the dynamic data in the linear viscoelastic region[37]:

$$G(t) = [G'(\omega) - 0.4G''(\omega) + 0.014G''(10\omega)]_{\omega=1/t} \quad (2)$$

t is the observed time. It can be seen from the calculated results, as shown by the solid line in Figure 7, that the calculated data were close to the experimental data. Moreover, there existed some deviation between the calculated and the experimental data. We believe that the long-time data of stress relaxation were responsible for the low-ω data of dynamic ω sweep. Although both kinds of data reflected the same viscoelastic essence, the response at low ω to external stimulation was highly sensitive compared to that of the long-time relaxation because of the complex structure of the blends. In addition, because of the differences in the polarity and molecular structure of the pure components, the blends were thermodynamically inhomogeneous systems. The degree of inhomogeneity depended on the graft ratio and composition of the blends. High inhomogeneity gave rise to high deviation between the calculated and experimental data.

In the linear viscoelastic range, $G(t)$ can be simulated by the Maxwell model as follows:

$$G(t) = \sum_{i=1}^{n} G_i e^{-(t-t')/\lambda_i} = \sum_{i=1}^{n} a_i \lambda_i e^{-(t-t')/\lambda_i} \quad (3)$$

where t is the observed time, G_i and λ_i are the modulus and relaxation time of the ith relaxation mode, respectively. The best fitting values of G_i and λ_i are summarized in Table I, and the corresponding results are shown by dashed lines in Figure 7. The values of G_i did not exhibit some rules with the

TABLE I
G_i and λ_i Values for the Nylon 1212/SEBS-*g*-MA Blends

	G_i (Pa)							
λ_i (s)	100/0	90/10	80/20	70/30	60/40	50/50	40/60	0/100
10^{-2}	393,300	198,969.4	336,515.8	276,117.8	164,118.5	228,451.3	121,835.2	230,213.2
10^{-1}	14,926.4	23,649.5	51,952.8	47,471.9	29,449.8	63,322.1	82,409.7	72,366.9
10^{-0}	1,288.6	1,069.5	2,028.9	2,048.7	2,196.4	5,481.7	13,043.4	6,780.8
10^{1}	75.58	236.7	2,262.9	3,375.3	3,350.3	5,802.9	8,658.1	6,190.5
10^{2}	5.21	17.4	161.2	1,508.2	1,633.2	2,731.0	4,790.4	4,670.7
10^{3}		12.0	622.4	3,335.8	2,867.5	2,227.9	6,504.8	1,181.2
10^{4}			1,518.4	1,727.8	6,769.1	5,662.8	9,736.5	

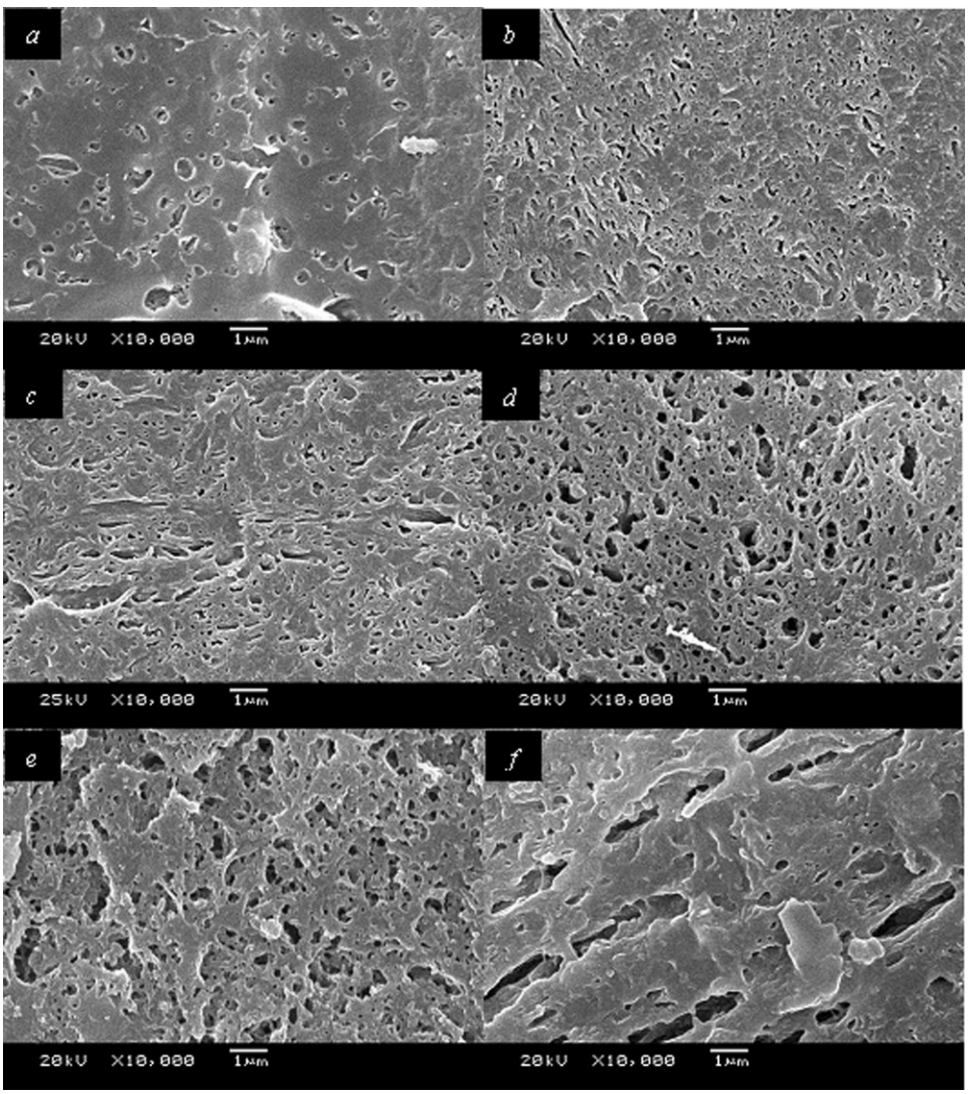

Figure 8 SEM images of cryofractured and boiling-xylene-etched surfaces of blends with various nylon 1212/SEBS-*g*-MA weight ratios: (a) 90/10, (b) 80/20, (c) 70/30, (d) 60/40, (e) 50/50, and (f) 40/60.

concentration increasing because of the complex structure of the blends. Furthermore, the simulated curve could describe the relaxation process of SEBS-*g*-MA well in the wide time range, but in the bottom, all of the fitting curves deviated from the experiment curves. The reasons for these were that, for nylon 1212 and the blends with 10 wt % SEBS-*g*-MA, the experimental data could not reflect the real relaxation process because of the scattering of the data, whereas for other blends and the pure elastomer, the Maxwell model was deduced from the experiment of the homogeneous polymer and could not completely describe the complex relaxation behavior of the blends and other systems with complex structures.

Morphology analysis of the blends

The viscoelastic behaviors of polymer systems can sensitively reflect differences in their morphologies, and the morphologies directly determine the complex viscoelastic behavior of polymer systems. Therefore, it is necessary to analyze the morphology of blends to understand their rheological behaviors more clearly. According to the SEM images of etched surfaces of the blends, as shown in Figure 8, we believe that nonreactive SEBS-*g*-MA phases were extracted from the broken surfaces on boiling with xylene for 12 h, and the images of SEM reflected the distributions of the elastomeric phases.

When the concentration of elastomer was relatively low, the elastomer was the dispersed phase and was distributed relatively orderly in the matrix of nylon 1212 [Fig. 8(a)], and the shape of the elastomer was incompletely spherical. Moreover, the globules were more or less uniform, the edges of the holes were relatively coarse, and the distance between two elastomeric particles was relatively far, which indicated that the interaction between the

dispersed phases was weak. We suggest that the addition of elastomer hardly affected the rheological behaviors of the matrix. Therefore, the rheological behaviors of the blends with 10 wt % elastomer were mainly controlled by the virgin nylon 1212. In the case of blends with 20 and 30 wt % SEBS-*g*-MA, the number of dispersed particles in the same unit area increased, and the morphologies of the blends were still droplet–matrix type, but the shapes of the particles were ellipsoid or irregular spheres, which meant that the blends entered gradually into the phase-transition region [Fig. 8(b,c)]. Accordingly, the rheological behaviors changed to some extent, which can be seen from the plots of the dynamic modulus versus composition of the blends (Fig. 4). With further increases in the elastomer concentration, the elastomeric particles agglomerated with each other and formed an interlocking phase morphology, but other particles still retained dispersed morphologies, and the densities and sizes of the holes became obviously larger [Fig. 8(d)]. When the concentration of SEBS-*g*-MA was 50 wt %, the morphology of the blend exhibited an obvious double-phase cocontinuity structure, although there were still some spherical particles distributed in the surface [Fig. 8(e)]. In addition, as shown in Figure 8(f), the nylon 1212 formed a dispersed phase, and the elastomer acted as the continuous phase, which corresponded to the results of the ω sweep tests (Fig. 3). On the basis of the previous analysis, we concluded that there was an obvious phase inversion when φ of the elastomer was near 50 wt %.

CONCLUSIONS

We carried out studies on the linear viscoelastic behaviors of nylon 1212 toughened with SEBS-*g*-MA elastomers. The results show that the critical shear strain of nylon 1212 was higher than that of pure SEBS-*g*-MA because the structure of the styrene block copolymer was a microphase separation structure and belonged to a heterogeneous structure, which was more easily destroyed by the accumulative strain history. Moreover, the plateau modulus of the blends in the curves of G' versus γ was higher than those of the virgin components, which was attributed to the improvement of entanglement molecular weight because of the graft reaction between the amine end groups of nylon 1212 and the maleic anhydride groups in SEBS-*g*-MA. On the other hand, all of the blends, except the one with 10 wt % SEBS-*g*-MA, displayed the second-plateau phenomenon in the G'–ω curves at low ω values, which was also attributed to the entanglement of longer macromolecular chains formed through the graft reaction.

The positive deviation in the plots of G' versus blend composition demonstrated that the blends were still immiscible, although the graft reaction improved the compatibility of the blend components. Furthermore, from the theory of phase transition, the phase-inversion point for these blends was predicted to be about 50 wt % SEBS-*g*-MA, which was consistent with the morphology analysis of the nylon 1212/SEBS-*g*-MA blends. Also, plots of G' versus G'', that is, so-called Cole–Cole plots of modulus, showed that the addition of functionalized elastomer enhanced the elasticity of the blends, and the functional elastomer toughened the nylon 1212 effectively. Additionally, except the blend with 10 wt % SEBS-*g*-MA, the blends showed yield stress behavior. Finally, the blends showed complex relaxation behaviors, and the Ninomiya equation and Maxwell model gave good agreement with the relaxation data.

References

1. Xanthos, M. Reactive Extrusion; Hanser: Munich, 1992.
2. Baker, W. E.; Scott, C. E.; Hu, G. H. Reactive Polymer Blending; Hanser: Munich, 2001.
3. Folkes, M. J.; Hope, P. S. Polymer Blends and Alloys; Chapman & Hall: London, 1993.
4. Van Aert, H. A. M.; Van Steenpaal, G. J. M.; Nelissen, L.; Lemstra, P. J.; Liska, J.; Bailly, C. Polymer 2001, 42, 2803.
5. Jeon, H. K.; Zhang, J. B.; Macosko, C. W. Polymer 2005, 46, 12322.
6. Brien, C. P. O.; Rice, J. K.; Dadmun, M. D. Eur Polym J 2004, 40, 1515.
7. Sailer, C.; Handge, U. A. Macromolecules 2007, 40, 2019.
8. Ozkoc, G.; Bayram, G.; Bayramli, E. J Appl Polym Sci 2007, 104, 926.
9. Macaubas, P. H. P.; Demarquette, N. R. Polymer 2001, 42, 2543.
10. Souza, A. M. C.; Demarquette, N. R. Polymer 2002, 43, 3959.
11. Michio, O.; Junichiro, W.; Ken, N.; Toshio, N. Polymer 2005, 46, 4899.
12. Li, W. D.; Li, R. K. Y.; Tjongu, S. C. Polym Test 1998, 16, 563.
13. Bartczak, Z.; Argon, A. S.; Cohen, R. E.; Weinbergu, M. Polymer 1999, 40, 2331.
14. Holz, N.; Goizueta, G. S.; Capiati, N. J. Polym Eng Sci 1996, 36, 2765.
15. Jain, A. K.; Nagpal, A. K.; Singhal, R.; Gupta, N. K. J Appl Polym Sci 2000, 78, 2089.
16. Kohan, M. I. Nylon Plastic Handbook; Hanser: Munich, 1995.
17. Kumar, S.; Ramanaiah, B. V.; Maiti, S. N. Soft Mater 2006, 4, 85.
18. Lai, S. M.; Li, H. C.; Liao, Y. C. Eur Polym J 2007, 43, 1660.
19. Hassan, A.; Othman, N.; Wahit, M. U.; Wei, L. J.; Rahmat, A. R.; Ishak, Z. A. M. Macromol Symp 2006, 239, 182.
20. Kelnar, I.; Kotek, J.; Kapralkova, L.; Hromadkova, J.; Kratochvil, J. J Appl Polym Sci 2006, 100, 1571.
21. Huang, J. J.; Keskkula, H.; Paul, D. R. Polymer 2006, 47, 639.
22. Oshinski, A. J.; Keskkula, H.; Paul, D. R. Polymer 1996, 37, 4909.
23. Abhijit, J.; Bhowmick, A. K. Polym Degrad Stab 1998, 62, 575.
24. Oommen, Z.; Zachariah, S. R.; Thomas, S.; Groeninckx, G.; Moldenaers, P.; Mewis, J. J Appl Polym Sci 2004, 92, 252.
25. Kumar, C. R.; Nair, S. V.; George, K. E.; Oommen, Z.; Thomas, S. Polym Eng Sci 2003, 43, 1555.
26. Wang, X. D.; Li, H. Q. J Mater Sci 2001, 36, 5465.
27. Zheng, Q.; Zhao, T. J. Chin J Mater Res 1998, 12, 225.

28. Zheng, Q.; Yang, B. B.; Wu, G.; Li, L. W. Chem J Chin Univ 1999, 20, 1483.
29. Palierne, J. F. Rheol Acta 1990, 29, 204.
30. Bousmina, M.; Muller, R. J Rheol 1993, 37, 663.
31. Fetters, L. J.; Lohse, D. J.; Garcia-Franco, C. A.; Brant, P.; Richter, D. Macromolecules 2002, 35, 10096.
32. Du, M.; Gong, J. H.; Zheng, Q. Polymer 2004, 45, 6725.
33. Incarnato, L.; Scarfato, P.; Scatteia, L.; Acierno, D. Polymer 2004, 45, 3487.
34. Payne, A. R.; Whittaker, R. E. Rubber Chem Technol 1971, 44, 440.
35. Jafari, S. H.; Potschke, P.; Stephan, M.; Warth, H.; Alberts, H. Polymer 2002, 43, 6985.
36. Majumdar, B.; Keskkula, H.; Paul, D. R. Polymer 1994, 35, 1386.
37. Ferry, J. D. Viscoelastic Properties of Polymers; Wiley: New York, 1980.
38. Zheng, Q.; Cao, Y. X.; Du, M. J Mater Sci Lett 2004, 39, 1813.
39. Nandan, B.; Kandpal, L. D.; Mathur, G. N. J Polym Sci Part B: Polym Phys 2004, 42, 1548.
40. Santamaria, A.; White, J. L. J Appl Polym Sci 1986, 31, 209.
41. Roovers, J.; Toporowski, P. M. Macromolecules 1992, 25, 1096.
42. Yoshikawa, K.; Molanár, A.; Eisenberg, A. Polym Eng Sci 1994, 34, 1056.
43. Han, C. D.; Chuang, H. K. J Appl Polym Sci 1985, 30, 4431.
44. Han, C. D.; Yang, H. H. J Appl Polym Sci 1987, 33, 1199.